Supporting Information for: Gas diffusion through variably-saturated zeolitic tuff: implications for transport following a subsurface nuclear event

7 pages, including 3 tables and 7 figures.

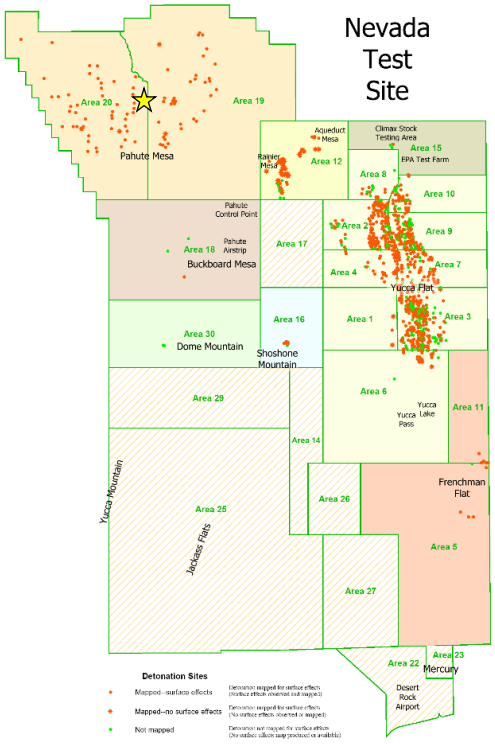

Figure S1. Map of NNSS. Samples were taken from Pahute Mesa in Area 20 (indicated by the yellow star).

Public domain image provided by Dennis N. Grasso, USGS and retooled from a USGS map called "Geologic Surface Effects of Underground Nuclear Testing, Buckboard Mesa, Climax Stock, Dome Mountain, Frenchman Flat, Rainier/Aqueduct Mesa, and Shoshone Mountain, Nevada Test Site, Nevada." (http://pubs.usgs.gov/of/2003/ofr-03-125/)

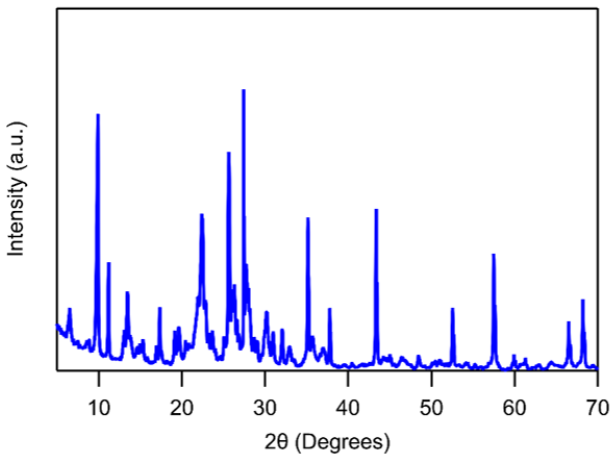

Figure S2. Quantitative XRD (QXRD) spectrum

Table S1. Porosity data for the NG-4 core. Zeolitic non-welded tuff (ZN) was used for diffusion experiments.

Lithology	Hole	Depth (ft)	Porosity (%)
RL	NG-4	900.7	2.6
SW	NG-4	240.5	8.8
PW	NG-4	28.8	29.3
PW	NG-6	12.7	25.4
PW	NG-4	128	12.8
VN	NG-4	470.3	1.1
SW	NG-4	67	12.3
VN	NG-4	764.6	23.4
ZN	NG-4	1285.7	16.7
ZN	NG-4	1513.9	19.2
ZN	NG-4	1680.4	22.6
ZN	NG-4	1341.4	16.8
ZN	NG-4	1376.0	32.7
SW	NG-4	228.8	7.1
RL	NG-4	946.8	0.3

PW=Partially Welded
SW=Strongly Welded
VN=Vitric Nonwelded
RL=Rhyolitic Lava
ZN=Zeolitic Nonwelded

Testing Xe Sorption: To calculate the approximate mass spec samples rate and test for preferential Xe sorption to plexiglass and silicone in the diffusion cell, we ran dilution tests for the three gases. For these tests, the diffusion cell chambers were sealed off by sandwiching just cured silicone between the two chambers. One chamber was spiked and then measured continuously using the mass spec. The drop in ion current indicated mass lost due to sampling and/or sorption. This slope was very similar for the three gases, with that of Xe being slightly lower (e.g., less mass lost), which indicates that there is no preferential Xe sorption on the chamber (Figure S3).

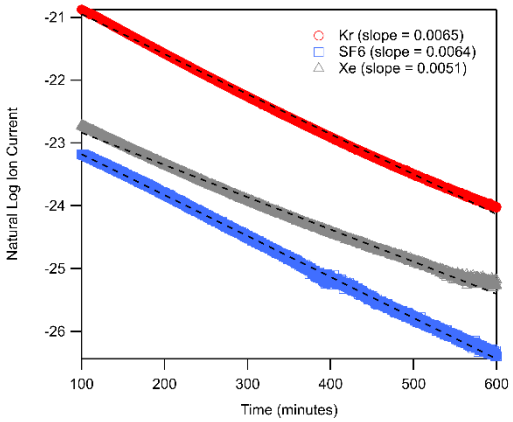

Figure S3. Natural log of ion current indicates mass lost from diffusion cell system. No preferential Xe sorption was observed.

Table S2. Los Alamos municipal tap water composition estimated by average groundwater measurements at the PM-1 well. Reprinted with permission from Neil *et al.* (2020).

Parameter Name	Report Result	Report Units	Parameter Name	Report Result	Report Units
pH	7.95	SU	Magnesium	6.02	mg/L
Alkalinity - CO_3	1.78	mg/L	Manganese	2.94	µg/L
Alkalinity - CO_3 + HCO_3	109.84	mg/L	Mercury	0.14	µg/L
Alkalinity - HCO_3	93.80	mg/L	Molybdenum	1.24	µg/L
Aluminum	68.86	µg/L	Nickel	0.84	µg/L
Ammonia as Nitrogen	0.07	mg/L	Nitrate - Nitrite as Nitrogen	0.49	mg/L
Antimony	0.91	µg/L	Perchlorate	1.42	µg/L
Arsenic	2.74	µg/L	Potassium	3.59	mg/L
Barium	73.43	µg/L	Rubidium	6.79	µg/L
Beryllium	1.41	µg/L	Selenium	2.22	µg/L
Bismuth	0.01	µg/L	Silicon Dioxide	76.95	mg/L
Boron	54.02	µg/L	Silver	0.35	µg/L
Bromate	0.00	mg/L	Sodium	19.39	mg/L
Bromide	0.14	mg/L	Specific Conductance	246.15	µS/cm
Cadmium	0.32	µg/L	Strontium	134.09	µg/L
Calcium	24.48	mg/L	Sulfate	5.02	mg/L
Cesium	0.04	µg/L	Tellurium	0.01	µg/L
Chlorate	0.00	mg/L	Thallium	0.56	µg/L
Chloride	6.00	mg/L	Thorium	0.01	µg/L
Chlorite	0.18	µg/L	Tin	10.37	µg/L
Chromium	4.21	µg/L	Titanium	0.08	µg/L
Cobalt	1.42	µg/L	Total Kjeldahl Nitrogen	0.07	mg/L
Copper	5.46	µg/L	Total Organic Carbon	0.65	mg/L
Fluoride	0.24	mg/L	Total Phosphate	0.04	mg/L
Gallium	0.05	µg/L	Tungsten	0.23	µg/L
Hardness	85.16	mg/L	Uranium	1.76	µg/L
Iodate	4.35	µg/L	Vanadium	11.73	µg/L
Iron	36.50	µg/L	Yttrium	0.01	µg/L
Lead	0.85	µg/L	Zinc	7.49	µg/L
Lithium	32.96	µg/L	Zirconium	0.03	µg/L

Neil, C.W., Telfeyan, K., Sauer, K.B., Ware, S.D., Reimus, P., Boukhalfa, H., Roback, R. and Brug, W.P., 2020. Iodine effective diffusion coefficients through volcanic rock: Influence of iodine speciation and rock geochemistry. *Journal of Contaminant Hydrology*, *235*, p.103714.

Table S3. Masses of rock cores used in diffusion experiments

Core A		**Core B**	
Mass (g)	*% Saturation*	*Mass (g)*	*% Saturation*
608.10	0% (Dry)	622.82	0% (Dry)
639.64	85%	628.83	17%
645.21	100% (Fully Saturated)	636.77	40%
		657.24	100% (Fully saturated)

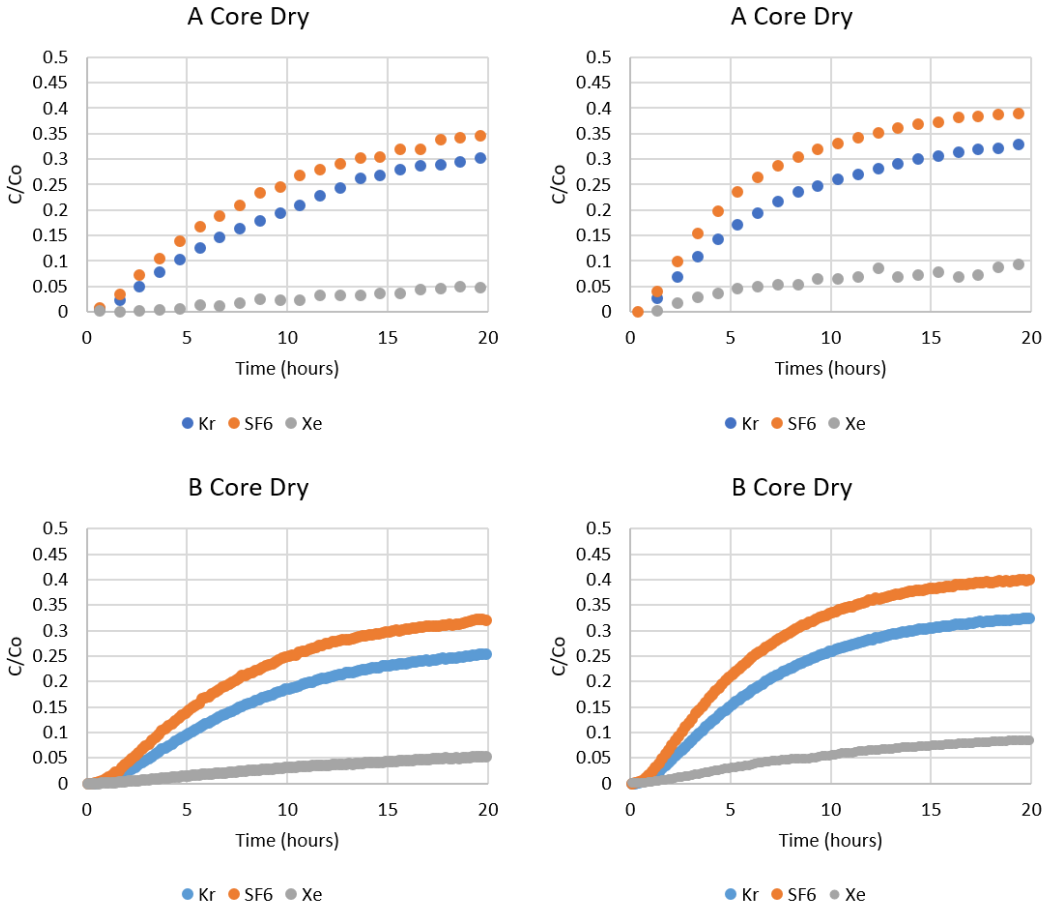

Figure S4. Dry breakthrough tests demonstrated reproducibility both between runs of the same core and between Core A and Core B.

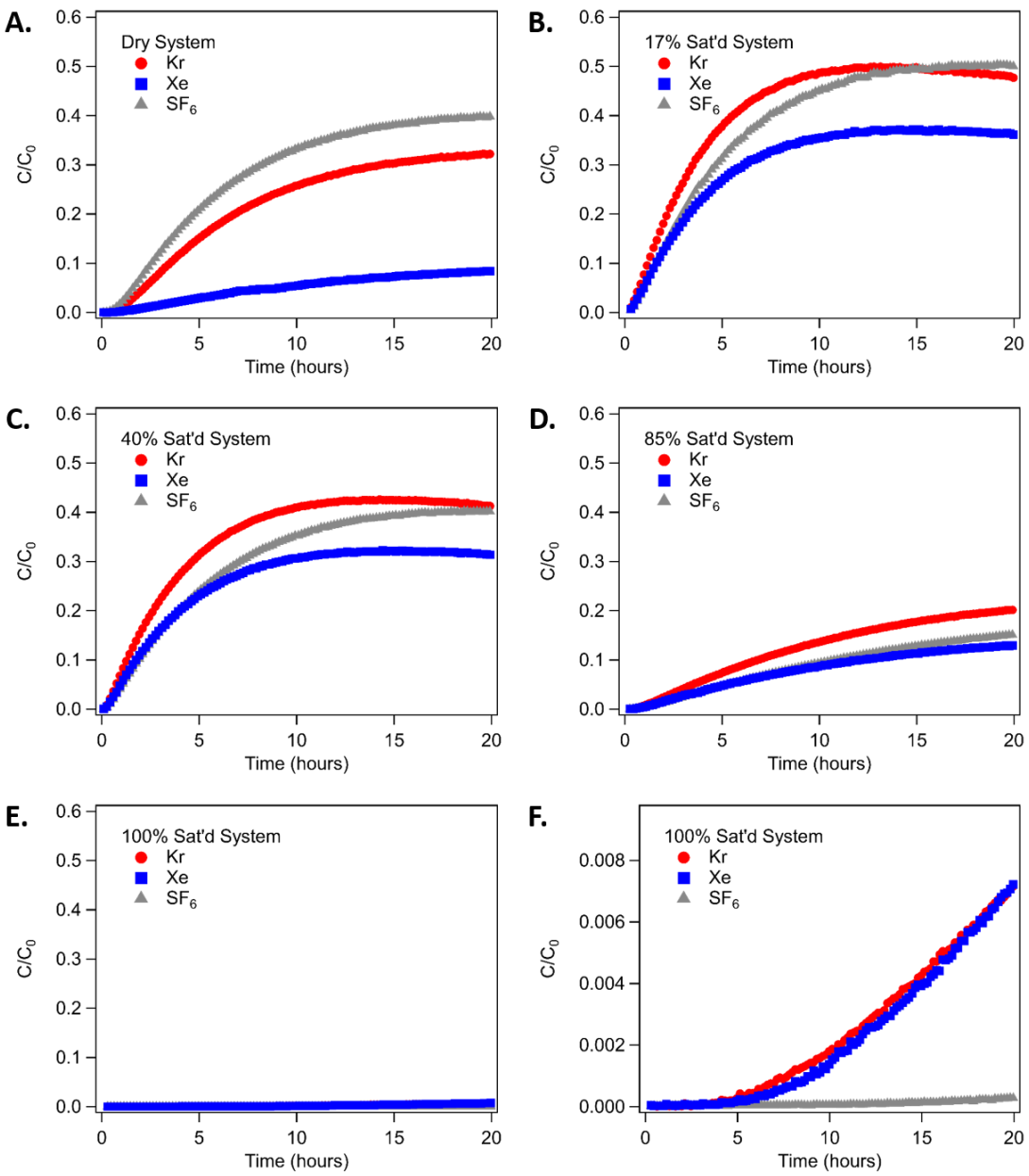

Figure S5. Twenty hour breakthrough comparisons for the (A) dry, (B) 17%, (C) 40%, (D) 85%, and (E) 100% saturated diffusion systems. (F) The 100% saturated system is zoomed in on the Y-axis to show breakthrough differences.

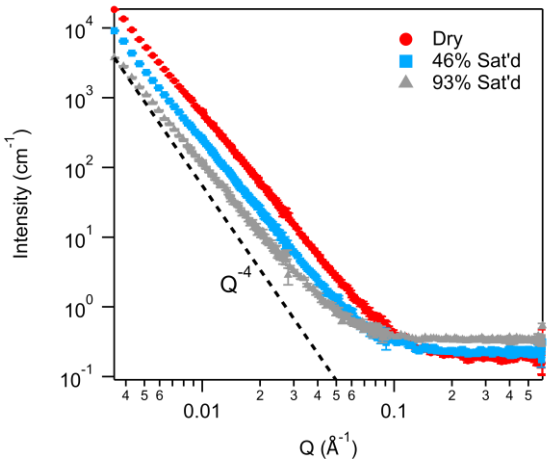

Figure S6. Reduced SANS spectra for tuff powder samples that were dry, exposed to 10 µL of water (46% saturated) and exposed to 20 µL of water (93% saturated). Intensity drop upon saturation occurs due to pore filling with contrast matched water. SANS spectra were fitted to determine pore size distribution differences between the three systems, indicating which pores are filled with water. Dotted line shows how pore scattering deviated from surface scattering (Q^{-4}). Fitted power laws are -3.33, -3.61, and -3.25 for the dry, 46% saturated, and 93% saturated tuff samples. The confidence internal is the standard deviation.

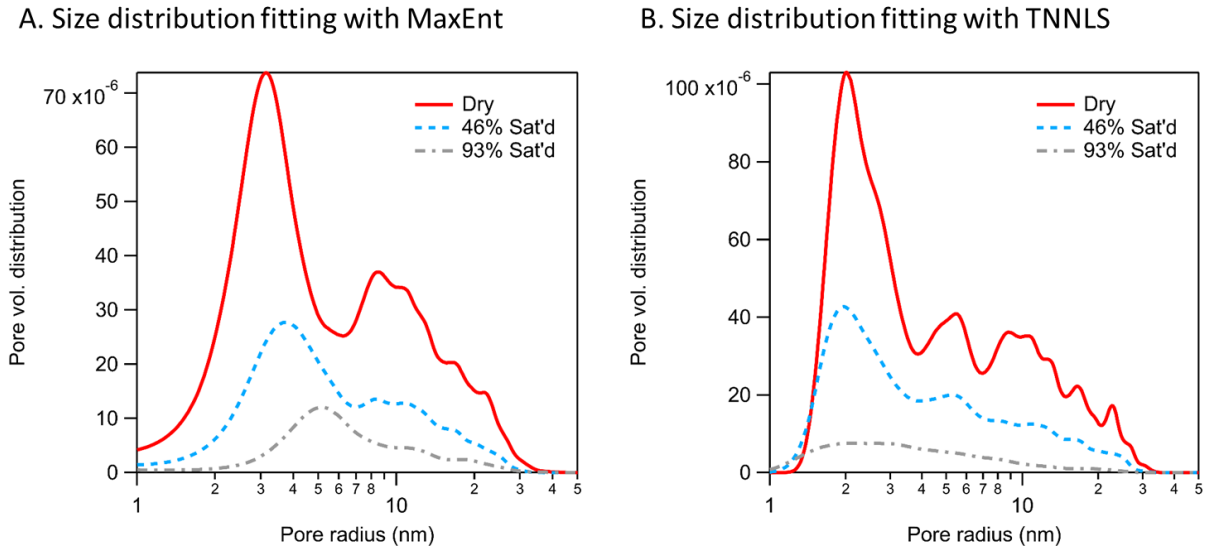

Figure S7. Comparison between Irena size distribution fitting using maximum entropy (MaxEnt, A) and total non-negative least squares (TNNLS, B). Both methods agree that upon partial saturation, the most significant drop in pore abundance occurred for the 3 nm radius pores.